

# **Population and decay from superdeformed states**

A. Lopez Martens

### 3. Population and decay from superdeformed states\*

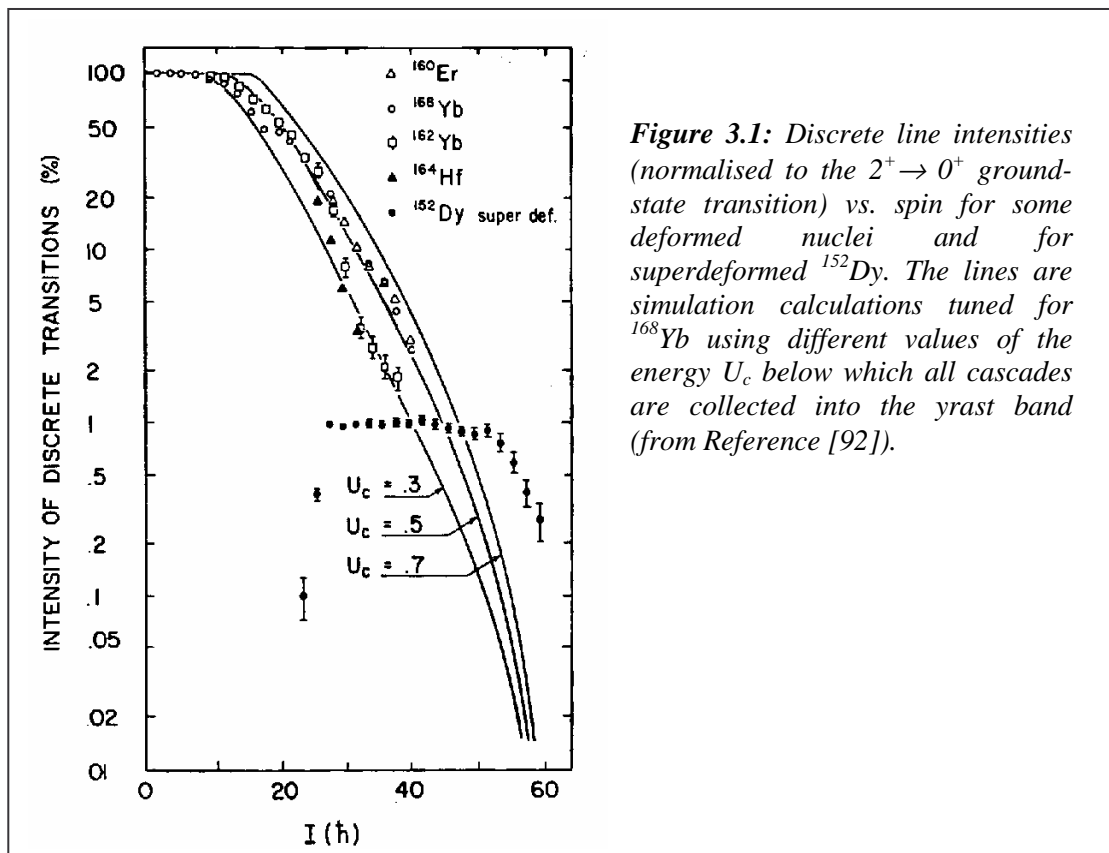
#### 3.1. Introduction

Superdeformed states are generally populated at high spin in fusion evaporation reactions but, in spite of numerous examples for superdeformed nuclei, the mechanisms governing their population are still not fully understood. The open questions concern the entrance channel effects, the enhanced cooling of superdeformed nuclei compared to normal-deformed nuclei and the transition from thermally excited motion to ordered regular rotation within the superdeformed well. The other topic of investigation is the decay from superdeformed states, which occurs very suddenly, in the space of 1-2 transitions. In the process, the nucleus gains a certain amount of deformation energy and cools down by emitting a series of gamma rays and in some cases, light particles. The questions here are what are the decay pathways in order to establish the excitation energies, spins and parities of superdeformed states, how the shape change occurs and more particularly how do superdeformed and normal-deformed states interact and mix and does the nucleus undergo a transition from ordered to chaotic motion?

#### 3.2. Population of superdeformed states

##### The E1 emission

The intensity of superdeformed yrast states is typically of the order of  $\sim 1\%$  of the fusion-evaporation channel. Albeit being small this value is still very large compared to what is extrapolated from the intensities of yrast states [92] (see Figure 3.1). One of the mechanisms



\* Contribution by A. Lopez-Martens

invoked to explain this enhancement is the enhanced E1 emission from the superdeformed nucleus [93] (cf. Section 4). This is due to the combination of two effects: the lower level density of superdeformed states and the splitting of the GDR built on superdeformed states which gives E1 strength at lower energies. In nuclei where the particle binding energy lies between 8-11 MeV, gamma emission can therefore compete more effectively with particle evaporation in a superdeformed nucleus than in a spherical one.

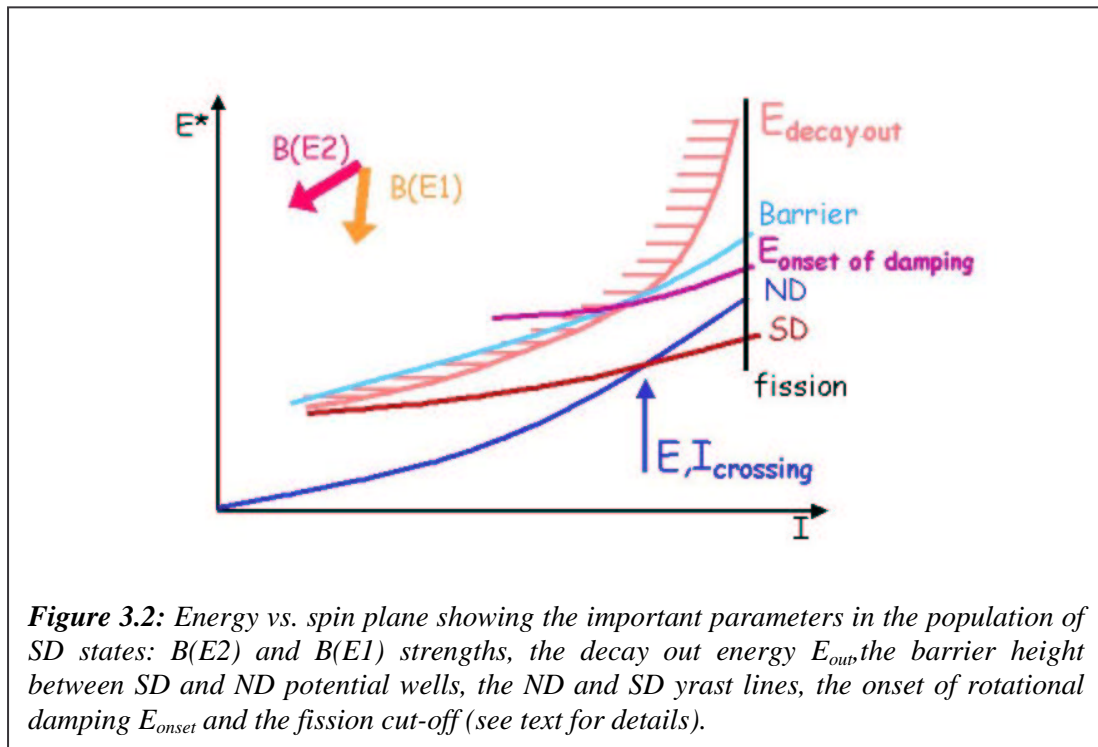
A recent experiment using EUROBALL and the BaF<sub>2</sub> HECTOR array (cf. Section 4) shows evidence for an excess intensity in the high energy part of the spectrum of gamma-rays detected with HECTOR in coincidence with superdeformed states in <sup>143</sup>Eu. This excess strength is observed at ~11 MeV, where one expects the low-energy component of the GDR. Inversely, superdeformed structures are enhanced when high-energy  $\gamma$ -rays are required in coincidence. All these experimental observations support the fact that instead of emitting a neutron, the superdeformed nucleus <sup>143</sup>Eu can emit a GDR photon and that high-energy E1 cooling is the preferred way to feed superdeformed structures [94,95].

The question that still needs to be addressed is whether this is a general feature of the population of superdeformed states or particular to the <sup>143</sup>Eu nucleus. Part of the answer to this question should be known quite soon from a EUROBALL experiment to study this feature also in <sup>196</sup>Pb.

### The E2 emission

As the nucleus cools down, E2 transitions start to compete with the E1 cooling and the question is where does the gamma flow go and what kind of superdeformed structures are sampled? The pattern of the regularly spaced E2 transitions of the yrast superdeformed structures is a very well known feature. Since the discovery of the first superdeformed rotational band in <sup>152</sup>Dy [13], more than 200 bands have been studied in nuclei of mass A~30, 60, 80, 130, 150, 160, 190 and the properties of the states which form the yrast superdeformed bands have shed light on many phenomena such as octupole vibrations, triaxial shapes and wobbling mode, C4 staggering, identical bands,... (cf. Sections 1 and 2). However, little is known about the E2 emission, which occurs at higher excitation energy. Only in one nucleus, <sup>143</sup>Eu, have these features been extensively studied. Two different E2 regimes have been identified [96] in this nucleus: (1) a very intense (~50%) ‘‘E2 bump’’, which is interpreted as being due to damped rotational transitions and (2) an intense ridge structure (~2%), which corresponds to the 2D correlation pattern from unresolved transitions that form excited discrete bands. Lifetime measurements at EUROBALL have firmly established their superdeformed nature [97]. A small damped continuum is seen in coincidence with the yrast superdeformed band, but no ridges are observed to feed the yrast superdeformed band. The number of discrete bands which contribute to the intensity of the ridges reflects the density of states at superdeformation, but it can also tell us something about the excitation energy at which rotational damping sets in and the magnitude of the rotational damping width. It was possible with EUROBALL to extract the number of discrete excited bands in <sup>143</sup>Eu and it was found that this number gradually decreases with spin [97] (cf. Section 4). This is well reproduced by theoretical calculations if the effect of mixing with normal-deformed states and subsequent decay-out is included in a broad spin and excitation energy range [98].

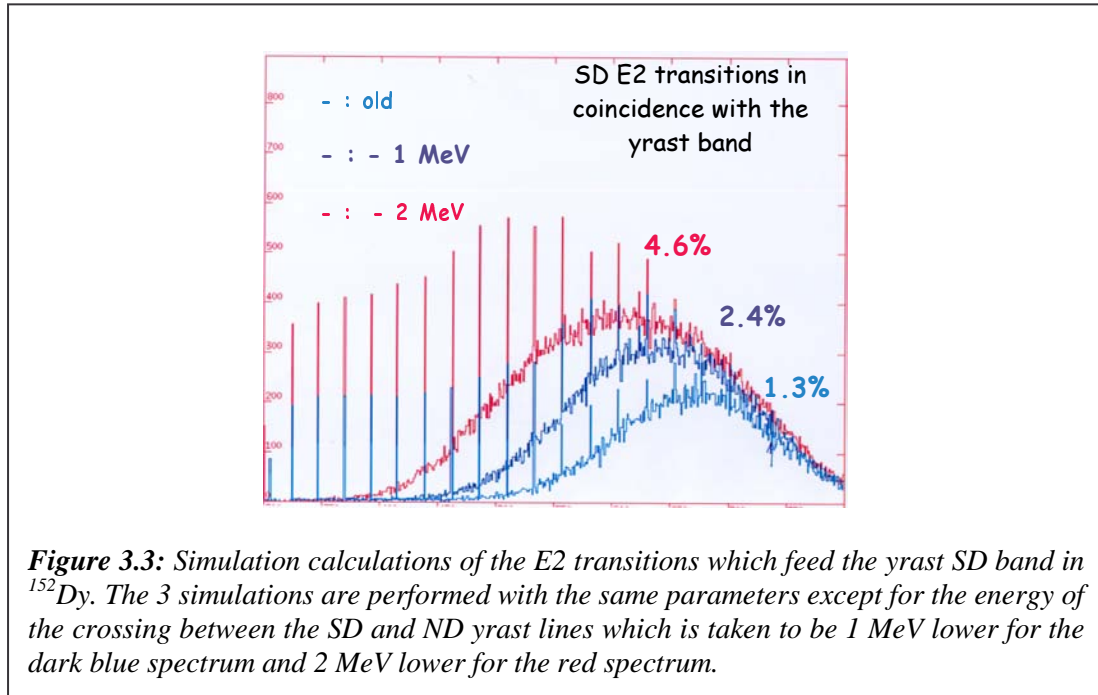
In other mass regions, there is little data available on this subject, but theoretical predictions exist and predict very different behaviours [99]. Because of the different shell structure involved in mass-190 superdeformed nuclei, the dispersion in frequency of the multi-particle



multi-hole states is considerably smaller when the spin changes by  $2\hbar$  than in the mass-150 region. This is why a much smaller rotational damping width  $\Gamma_{rot}$  is predicted, with the consequence that the onset of damping, or the onset of the fragmentation of the E2 strength over many final states will occur at higher excitation energy than the configuration mixing itself. One should therefore expect to observe more discrete bands (discrete in the sense little or no spreading out of the E2 strength). In some cases, these bands may even be ergodic bands [100]: regular bands built on compound states. Theory also predicts that the number of bands should decrease at high spin because of the decrease in the height of the barrier separating superdeformed and normal-deformed states. There are preliminary GAMMASPHERE results on this subject, but only a high-statistics experiment (as was recently performed with EUROBALL to study  $^{192}\text{Hg}$ ) will allow a detailed investigation of the feeding properties of the superdeformed nucleus as a function of temperature and spin.

The properties of the gamma flow in the second well depend on the energy vs. spin (E,I) landscape, which is drawn schematically in Figure 3.2. E2 transitions associated with superdeformed states can only exist between the superdeformed yrast line and the decay-out energy ( $E_{out}$ ). This region is further divided by the onset energy of damping ( $E_{onset}$ ); below  $E_{onset}$ , superdeformed states form regular rotational bands and above it, states decay by E2 transitions characteristic of the superdeformed shape, but the strength is fragmented over many final states. Where the flow will go and how much of it actually feeds into the yrast line will depend on the initial (E,I) distribution of the compound nucleus, on the magnitude of the  $B(E2)$  and  $B(E1)$  strengths at super- and normal deformation and on the relative positions of all the lines drawn in Figure 3.2, especially the relative position of the superdeformed and normal-deformed yrast lines.

Recently, the yrast band in  $^{152}\text{Dy}$  has been linked [101] into the rest of the level scheme of  $^{152}\text{Dy}$  and it turns out that the crossing point between the normal-deformed and superdeformed yrast lines is 1 MeV and  $10\hbar$  lower than previously thought. This has a dramatic influence on the simulation of the population of superdeformed (yrast and excited) and



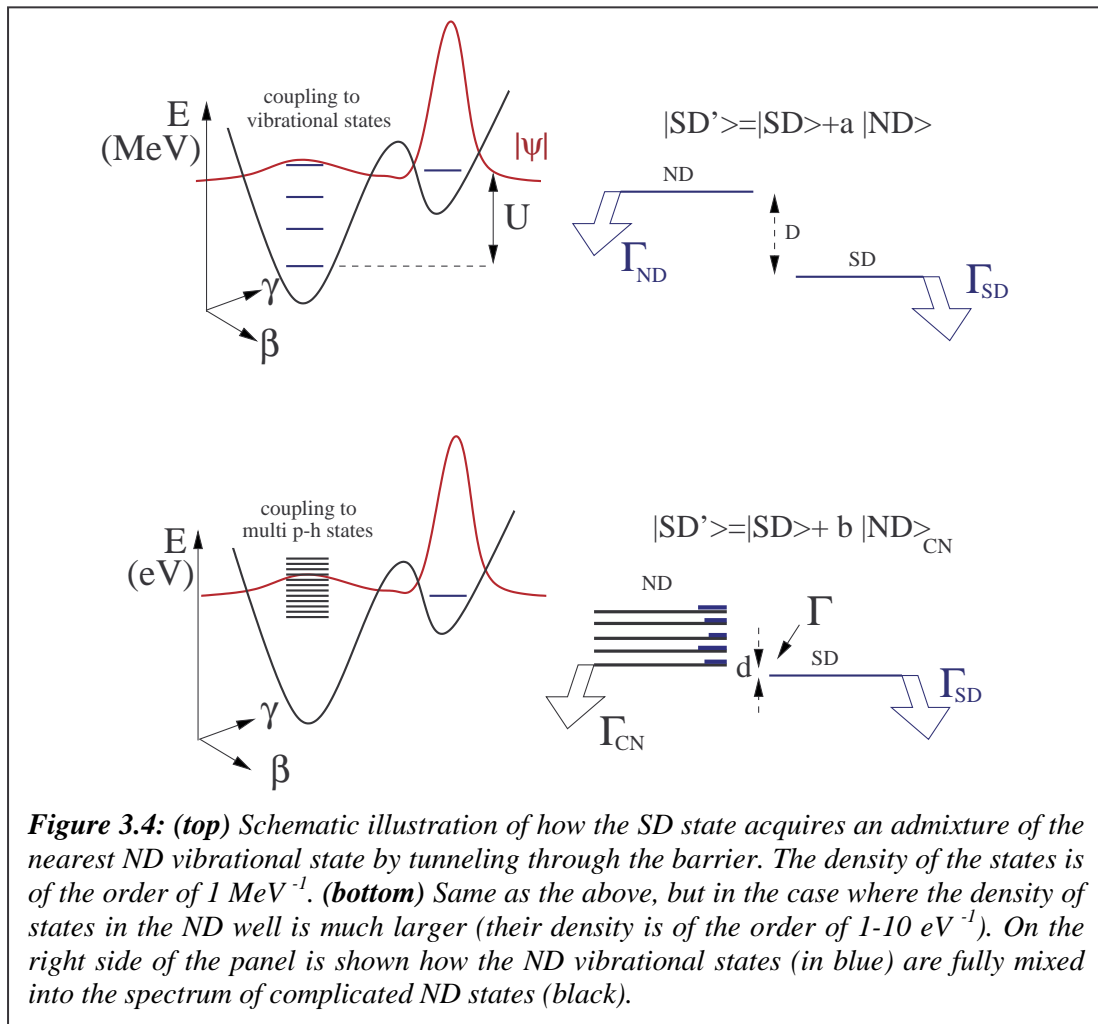
normal-deformed states. Indeed, as is shown in Figure 3.3, given a set of simulation parameters, if the superdeformed yrast line is lowered by 1 MeV, the population of the yrast superdeformed states increases from 1.3 to 2.4% and the superdeformed continuum (which is made up of damped transitions and the projection of the ridges) grows and is shifted to lower spin (the profile of the yrast band also moves down by 4  $\hbar$ ). A similar increase in intensity and a shift to lower spin occur when the excitation energy of the crossing point is lowered by another 1 MeV.

Much has been learnt on the different stages of the feeding of superdeformed states using EUROBALL, but it is clear that in order to understand the important parameters of the population process, one must first have a better knowledge on the decay-out properties of the superdeformed yrast states.

### 3.3. Decay from superdeformed states

The decay out of superdeformed bands is due to the coupling between superdeformed and normal-deformed states. The coupling or tunneling occurs in collective coordinate space by quadrupole couplings between the different configurations along the path between the superdeformed and normal-deformed minima. If the excitation energy of the superdeformed state is low, it will couple to the closest lying collective normal-deformed state and acquire an admixture of such a normal-deformed state (see Figure 3.4, top panel). This can be calculated in a fully microscopic way going beyond the mean field in order to take into account correlations and fluctuations (GCM approach [102]). The resulting state has then a partial E2 width ( $\Gamma_{\text{SD}}$ ) to decay to the next superdeformed state and a partial width ( $\Gamma_{\text{ND}}$ ) to decay out of the band, down to low energy normal-deformed states.

If, on the other hand, the excitation energy is such that the collective states (often called doorway states) on the normal-deformed side are fully mixed into a dense sea of very complicated multi-particle multi-hole excitations, and if the coupling is weak, the

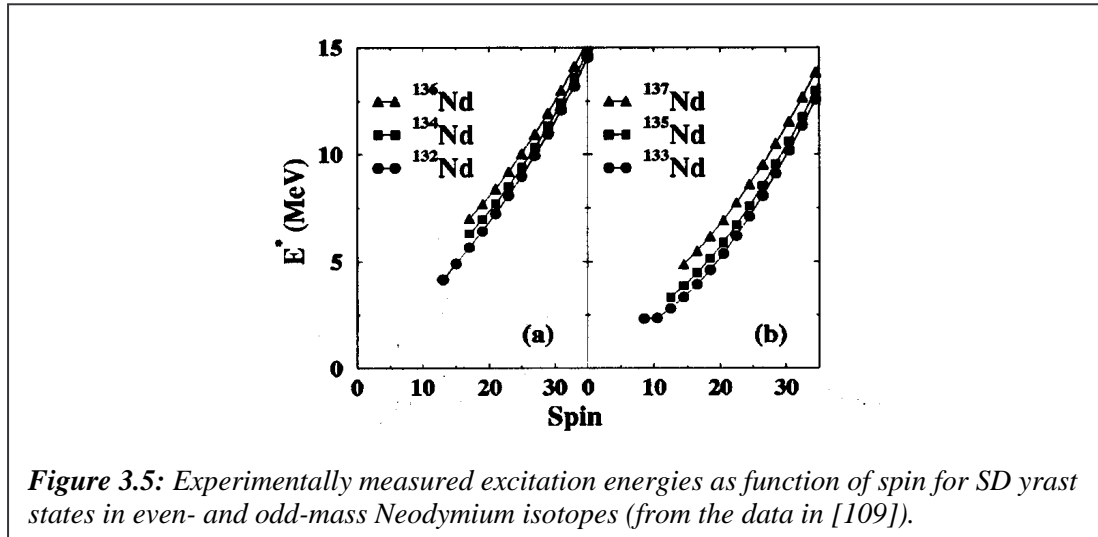


superdeformed state will couple to the closest compound state which has a statistical decay width ( $\Gamma_{\text{CN}}$ ) to decay down to low energy normal-deformed states (see Figure 3.4, bottom panel). This other extreme decay-out scenario can be calculated using micro-macroscopic models combined with statistical approaches [103,98].

### Excitation energy of superdeformed states

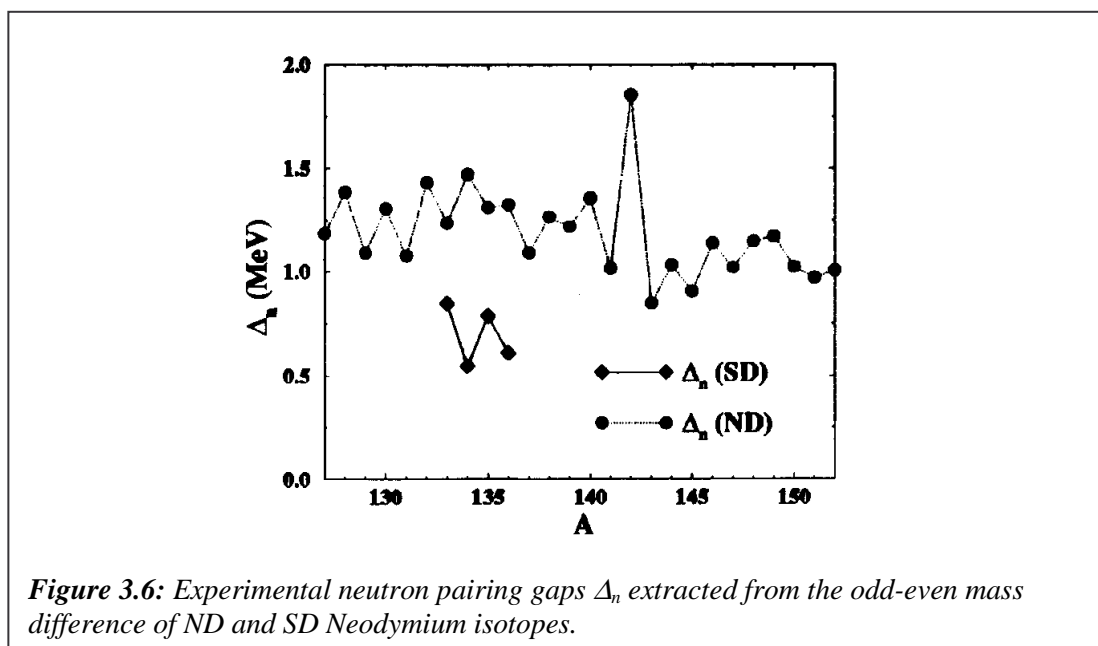
One can unambiguously determine the absolute energy, spin and parity of superdeformed states by identifying directly connecting pathways from the superdeformed state to known normal-deformed states. However, only a handful of superdeformed bands have been connected to the low-lying normal-deformed states. This is because in most of the cases, the density of final states for the decay is very large. The decay is consequently highly fragmented and the transitions, which directly connect superdeformed states to low-lying normal-deformed states, are high-energy  $\gamma$ -rays. It is therefore a difficult experimental task to observe these single-step links since their signal corresponds to  $\sim 10^{-4}$  of the reaction channel, not counting the reduced  $\gamma$ -ray efficiency at high energy and possible chaotic effects.

But in some cases nature is kind and the differences in configuration between superdeformed and normal-deformed states can be less pronounced and the excitation energy of superdeformed states smaller. This is the case of the Neodymium isotopes. The yrast superdeformed bands in  $^{132\text{-}137}\text{Nd}$  have all been connected to the corresponding normal-deformed level scheme [104-108]; the most recent case,  $^{136}\text{Nd}$ , was studied at EUROBALL [109]. As is



shown in Figure 3.5, the excitation energies of superdeformed states in six Nd isotopes are known as a function of spin. The value of the observed decay-out intensity is 100, 50 and 20% for  $^{132}\text{Nd}$ ,  $^{134}\text{Nd}$  and  $^{136}\text{Nd}$  and 100, 65 and 30% for  $^{133}\text{Nd}$ ,  $^{135}\text{Nd}$  and  $^{137}\text{Nd}$ , respectively. This decrease is related to the increase in the excitation energy of the superdeformed bands with neutron number: as  $N$  approaches 82, deformed structures are getting more costly in energy. Also, the excitation energy is systematically higher in the even systems than in the odd ones. This is related to the nature of the superdeformed configuration, which is two quasi-particle in the even cases and one quasi-particle in the odd cases.

From these data it was possible to extract the neutron pairing gap in the superdeformed well of Nd nuclei [109,110]: In the independent quasi-particle picture, and with some assumptions on the contribution of rotation to the excitation energy of the six superdeformed nuclei, one can relate the odd-even mass difference at spin  $I$  to an average neutron pairing gap  $\Delta_n$ . The values of  $\Delta_n$  plotted in Figure 3.6 for superdeformed matter are mean values extracted within the spin range of the bands. The error bars are large ( $\sim 50\%$ ) due to the approximations made and the uncertainties in the mass values. It is expected that  $\Delta_n$  should be reduced because of the blocking effect of the quasi-particles. This is estimated to be a 20% effect, but here the



quenching is stronger. Pairing correlations are therefore reduced but the most important result is that they still exist in mass-130 superdeformed nuclei at relatively high spins.

### Coupling between superdeformed and normal-deformed states

Another new result concerning the decay out comes from the triaxial superdeformed bands in  $^{163}\text{Lu}$ . The yrast superdeformed states (band TSD1) to which the excited, so-called “wobbling” band [58] decays have been connected to the lower lying states [72]. In fact, there is a very strong interaction between the superdeformed state and a neighbouring normal-deformed state at spin  $21/2\hbar$ . The superdeformed  $21/2^+$  state acquires a small admixture of the normal-deformed  $21/2^+$  state and vice versa. As can be seen in Figure 2.5 (cf. Section 2), the superdeformed transition  $25/2^+ \rightarrow 21/2^+$  is actually split into two transitions of 315 and 427 keV, respectively. The normal-deformed and superdeformed  $21/2^+$  states will be fed from the  $25/2^+$  superdeformed state proportionally to their squared superdeformed amplitudes,  $\alpha^2$  and  $(1-\alpha^2)$  respectively. From the experimental intensity and B(E2) ratios, a value of  $\sim 4\%$  was extracted for  $\alpha^2$ . This is of the order of what one obtains in the mass 190 and 150 regions assuming a statistical decay. The unperturbed energies of band TSD1 can then be derived and the dynamical moment of inertia recalculated.

Figure 3.7 shows the moments of inertia using the experimental energy differences between 2 consecutive transitions (filled circles) and the energy differences, which result when the level shift due to the mixing at spin  $21/2\hbar$  is removed (open circles). As in the  $^{133}\text{Nd}$  case, the irregularities of the moment of inertia disappear. The interaction strength between the superdeformed and normal-deformed states is large (22 keV). Similar values are found in the Nd isotopes. In mass 150 and 190 nuclei this interaction is estimated to be of the order of 1 to a few eV. This is because the difference between normal-deformed and superdeformed configurations is much larger and many more particles have to be rearranged to go from one configuration to the other.

This rearrangement of particles involved in the decay-out process is also nicely supported by the observations of “scaled” decay-out strengths in  $^{58}\text{Cu}$  [111] (cf. Section 7). Indeed, the E2 strengths of the 830, 1519 and 4171 keV transitions depopulating the  $(11^+)$  second minimum state in  $^{58}\text{Cu}$  scale as  $0.1^N$ ;  $N=0,2,4$  being the number of particle-hole excitations which are to

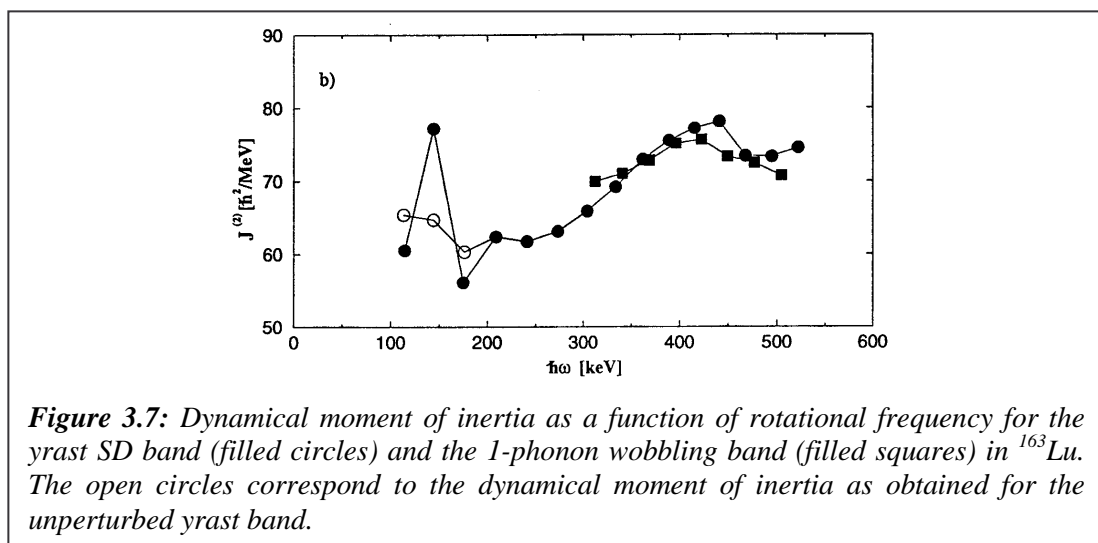


**Figure 3.7:** Dynamical moment of inertia as a function of rotational frequency for the yrast SD band (filled circles) and the 1-phonon wobbling band (filled squares) in  $^{163}\text{Lu}$ . The open circles correspond to the dynamical moment of inertia as obtained for the unperturbed yrast band.

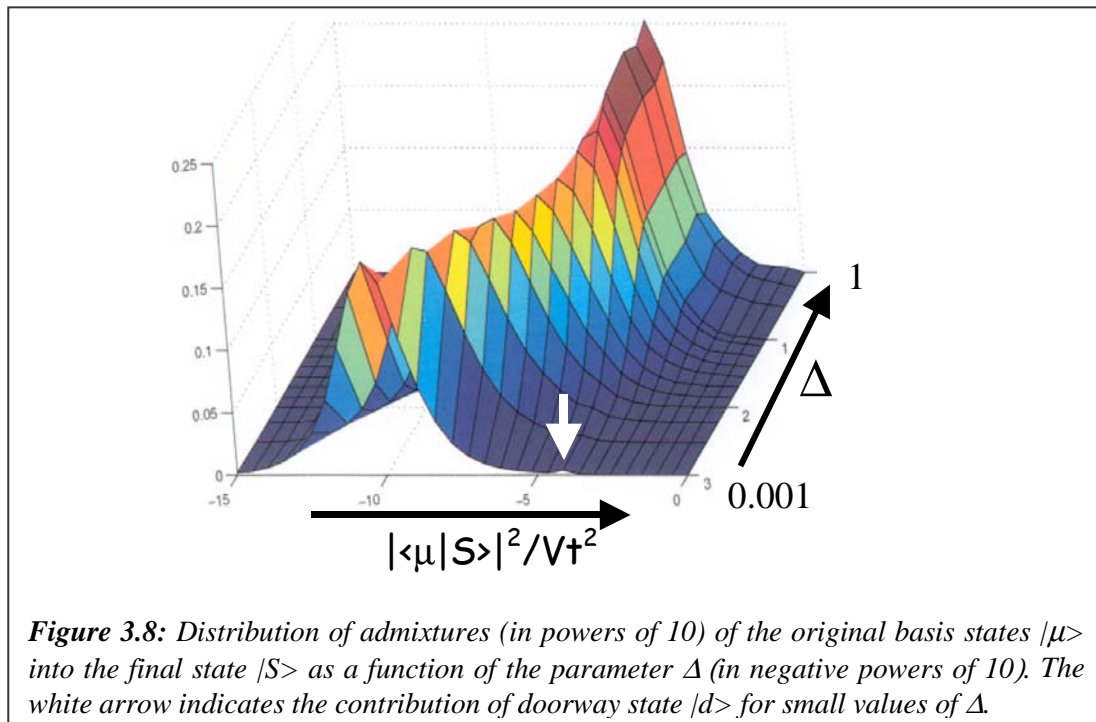
be reconfigured. The  $\gamma$  decay-out strengths are based on lifetime measurements of individual states, which were performed for the first time in the A=60 mass region using EUROBALL.

### Primary decay-out strength distribution

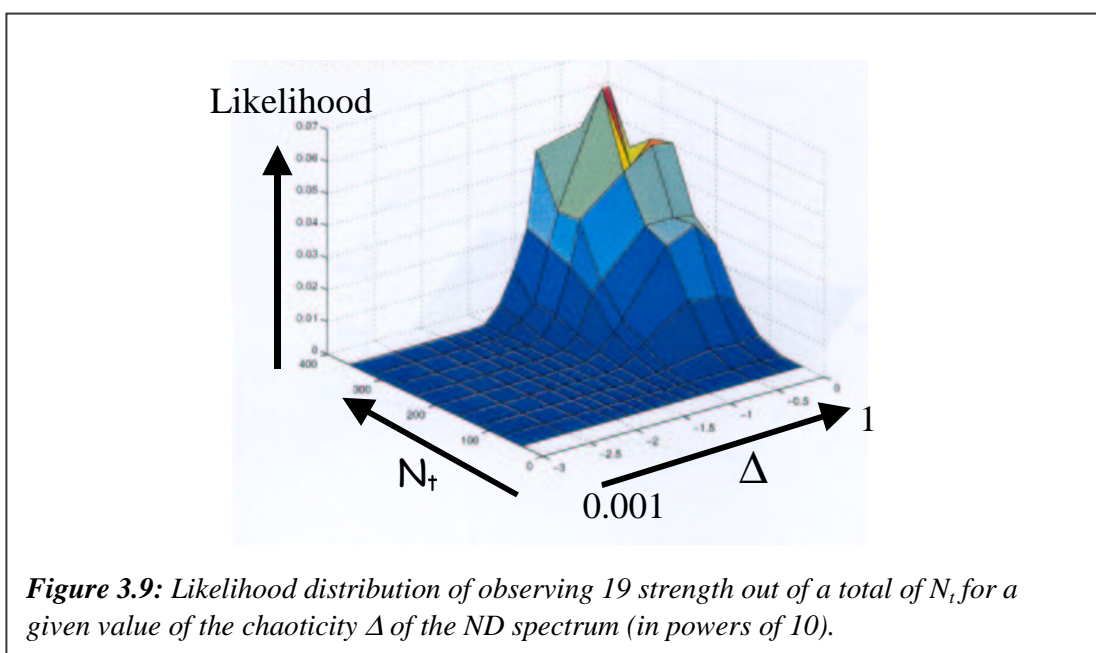
In the cases where the excitation energy of the superdeformed nucleus and the density of normal-deformed states at the point of decay are very large, the superdeformed state couples to the nearest compound state and the decay-out should be typical of the decay of a hot compound state. It should be made up of a broad bump corresponding to the pileup of primary and secondary and may be tertiary transitions leading the nucleus down to the yrast states, the yrast transitions and the single-step links which sit close to the endpoint of the spectrum. As in the neutron resonance case [112], the primary transition strengths should follow a  $\chi^2$  distribution with  $\nu=1$  degree of freedom, often called Porter-Thomas distribution [113]. This is a direct consequence of random matrix theory and more specifically, it reflects the properties of the Gaussian Orthogonal Ensemble of matrices (GOE). This gives rise to very strong strength fluctuations which could be the reason why single-step links are sometimes enhanced and can be observed experimentally. This is the case in  $^{194}\text{Hg}$ , for which strong high-energy links have been identified [114,25] while in the neighbouring  $^{192}\text{Hg}$ , studied with similar statistics, no such lines could be observed.

In order to verify that the enhancement of the strengths in  $^{194}\text{Hg}$  is due to Porter-Thomas fluctuations, a study of the primary strength distribution was performed [115]. The aim was to determine which  $\chi^2$  distribution of  $\nu$  degrees of freedom and average strength  $\theta$  could best fit the experimental strengths  $\omega_i$  above the experimental strength threshold  $\omega_{\text{low}}$ . The result for the most likely  $\chi^2$  distribution is the following:  $\nu = 1$  and  $\theta$  is found to be nearly 4 times smaller than the experimental strength threshold. The uncertainty on  $\nu$  is very large because only the high-strength tail of the distribution is accessible experimentally and this is a strength domain for which there is not a pronounced difference between  $\chi^2$  distributions. In other words, only the strongest 19 strengths are observed, whereas a fluctuation analysis in the same energy range tells us there should be  $\sim 600$  (primary) transitions.

In order to apply this method, more primary  $\gamma$ -rays need to be identified. This can be done in the cases where the phase space for the decay-out transitions is more favourable and the primary lines more intense. The problem, however, in dealing with  $\chi^2$ -distributions is that only the  $\nu=1$  distribution has a well-defined meaning. In order to overcome this problem, a formalism developed by Sven Åberg [116] was used. This method introduces a ‘‘chaoticity’’ parameter and since it is no longer analytical, it requires simulations. The spectrum of normal-deformed states is constructed from a GOE matrix of size  $N$ . One of the basis states  $|\mu\rangle$  is special since it can couple to the superdeformed state. This state is named  $|d\rangle$  for doorway. The off-diagonal elements of the matrix, which govern the mixing between the normal states, are scaled with a parameter  $\Delta$  ( $0 \leq \Delta \leq 1$ ). After a first diagonalisation procedure, the superdeformed state  $|SD\rangle$  is included together with its coupling  $V_t$  to the doorway state and another diagonalisation is carried out. When the parameter  $\Delta$  is 0, the ND states do not interact with each other and the superdeformed state can only acquire an admixture of the doorway state. When  $\Delta$  is equal to 1, the normal-deformed spectrum is fully mixed, the doorway state has dissolved among all the normal-deformed states and since the coupling  $V_t$  is weak, one of the final states  $|S\rangle$ , which has a predominant superdeformed component, will include many small admixtures of the original normal-deformed states  $|\mu\rangle$ .



In the plot of the distribution of these admixtures into the final state  $|S\rangle$  as a function of  $\Delta$  (Figure 3.8), it is immediately clear what is meant by “chaos-assisted tunneling”. At small  $\Delta$ , the admixture into  $|S\rangle$  is mostly due to the doorway state at an arbitrary value of  $10^{-5}$ . At  $\Delta = 1$ , all the  $N$  basis states will contribute on average with one admixture of that order: the admixture of normal-deformed states into the superdeformed state is  $\sim N$  times larger in the chaotic limit than in the ordered limit. To proceed further, the conjecture is that admixtures can be viewed as strengths.  $N_s$  simulations are carried out. For each simulation,  $N_t$  strengths are randomly chosen. Out of these  $N_t$  strengths, the  $N_o$  strongest (o for observed as in the experiment) are selected.



The smallest of these  $N_0$  strength is then equivalent to the experimental strength threshold and all the strengths are normalised to it. As in the  $\chi^2$  case, the likelihood that the 19 experimental strengths correspond to 19 strengths sampled from a total of  $N_t$ , given a value of  $\Delta$  can be plotted. In Figure 3.9 the preliminary results for the  $^{194}\text{Hg}$  nucleus are shown. Each point in the plot corresponds to the average of 500 different GOE matrices of size 400 and subsequent diagonalisations and the strength threshold is given by the observation of 19 strengths. The likelihood to observe 19 strengths is peaked when the total number of primary strengths is larger than 200 and when  $\Delta$  is larger than 0.1. This is in agreement with the measurement of 600 primary lines in the transition energy range from 2.6 to 5 MeV and with the result of the most likely  $\chi^2$  distribution. It therefore appears highly probable that the decay-out in  $^{194}\text{Hg}$  is a statistical process and that the normal-deformed states to which the superdeformed states couple to at 4.2 MeV above yrast are compound states.

### 3.4. Conclusion

Excited states within a superdeformed well provide opportunities to investigate many intriguing nuclear structure aspects: a transition from ordered motion along the superdeformed yrast line to chaotic motion above, perhaps through an ergodic regime; the robustness of collectivity with increasing excitation energy and spin and the largely-unexplored feeding mechanism of superdeformed bands. A very extensive study of superdeformed excited states has been carried out in  $^{143}\text{Eu}$  and a clear picture of the feeding process in this nucleus is emerging. Theoretical calculations predict different phenomena in other mass regions and experiments to study mass 190 and 150 nuclei have recently been performed and are still being analysed.

Concerning the decay-out, most bands are still not connected to the low-lying levels. This is because experiments are at the very limits of what present arrays can do. In the few cases where quantum numbers have been measured for superdeformed states, information on binding energies and pairing in the second minimum has been extracted as well as values for the interaction strength between superdeformed and normal-deformed states. The decay-out is also a tool to study the nature of normal-deformed states in a large (E,I) domain and methods have been developed to exploit this. Finally, and this was not mentioned, considerable effort has been done at EUROBALL to study the conversion-electron and possible E0 decay-out spectrum in  $^{136}\text{Nd}$  and  $^{194}\text{Pb}$ . However, these experiments are very difficult and no results could be obtained so far.

The near future of  $\gamma$ -ray spectroscopy in the superdeformed well and its future in general look rather bright. Indeed, several experiments recently performed with EUROBALL are still being analysed and will reveal new and exciting physics. On a longer time scale, the new generation of  $4\pi$   $\gamma$ -ray spectrometers such as AGATA, combined with intense stable and radioactive beams, will no doubt allow us to revisit superdeformation and discover more exotic nuclear shapes.

### Acknowledgements

The author would like to thank T. Døssing, B. Herskind, T.L Khoo, S. Åberg, F. Camera, S. Leoni and the nuclear structure group of CSNSM for fruitful discussions and for helping to prepare the presentation and the contribution.